Spectrochimica Acta Part A 86 (2012) 8–14

Spectrochimica Acta Part A: Molecular and Biomolecular Spectroscopy

journal homepage: www.elsevier.com/locate/saa

Enhanced photoluminescence of Gd_2O_3:Eu^{3+} nanophosphors with alkali ($M = Li^+$, Na^+, K^+) metal ion co-doping

N. Dhananjaya[a,b], H. Nagabhushana[c,*], B.M. Nagabhushana[d], B. Rudraswamy[a], C. Shivakumara[e], K. Narahari[f], R.P.S. Chakradhar[g]

[a] Department of Physics, J.B. Campus, Bangalore University, Bangalore 560 056, India
[b] Department of Physics, B.M.S. Institute of Technology, Bangalore 560 064, India
[c] Prof. C.N.R. Rao Centre for advanced Materials Research, Tumkur University, Tumkur 572 103, India
[d] Department of Chemistry, M.S. Ramaiah Institute of Technology, Bangalore 560 054, India
[e] Solid State and Structural Chemistry Unit, Indian Institute of Science, Bangalore 560 012, India
[f] Centre for Advanced Materials (CAM), Tumkur University, Tumkur 572 103, India
[g] National Aerospace Laboratories (CSIR), Bangalore 560017, India

ARTICLE INFO

Article history:
Received 10 February 2011
Received in revised form 16 May 2011
Accepted 24 May 2011

Keywords:
Nanophosphor
Gadolinium oxide
Co-dopant
XRD
SEM
FTIR
Photoluminescence

ABSTRACT

$Gd_{1.95}Eu_{0.04}M_{0.01}O_3$ ($M = Li^+$, Na^+, K^+) nanophosphors have been synthesized by a low temperature solution combustion (LSC) method. Powder X-ray diffraction pattern (PXRD), scanning electron microscopy (SEM), UV–vis and photoluminescence (PL) measurements were carried out to characterize their structural and luminescent properties. The excitation and emission spectra indicated that the phosphor could be well excited by UV light (243 nm) and emit red light about 612 nm. The effect of alkali co-dopant on PL properties has been examined. The results showed that incorporation of Li^+, Na^+ and K^+ in to Gd_2O_3:Eu^{3+} phosphor would lead to a remarkable increase of photoluminescence. The PL intensity of Gd_2O_3:Eu^{3+} phosphor was improved evidently by co-doping with Li^+ ions whose radius is less than that of Gd^{3+} and hardly with Na^+, K^+ whose radius is larger than that of Gd^{3+}. The effect of co-dopants on enhanced luminescence was mainly regarded as the result of a suitable local distortion of crystal field surrounding the Eu^{3+} activator. These results will play an important role in seeking some more effective co-dopants.

1. Introduction

It is well known that luminescent efficiency of phosphors can be enhanced by modifying their compositions. It has been reported that sometimes even very small quantities of co-dopants can lead to a great improvement of luminescent efficiency of phosphors [1]. Recently, there has been significant research on the development of high efficient phosphors with the incorporation of rare earth co-dopants or non rare earth dopants in to phosphors [2,3]. The role of rare earth co-dopants is generally related to the process of energy transfer, up conversion and cross relaxation [4]. Contrary to that, the role of non-rare earth co-dopants is yet to be confirmed. Consequently, several effects of non-rare earth co-dopants, which are believed to be responsible for the increase of luminescence efficiency has been the subject of recent interest.

Alkali elements such as Li^+, Na^+, and K^+ were selected as co-doping ions because of their wide application in luminescent host materials [5]. Since the ionic radius and charge state of alkali metal ions are different from those of host (Gd^{3+}), the crystal lattice would be distorted, and the high symmetry around Eu^{3+} site can be destroyed and a better color parity can be achieved [6]. In our prior work, the Eu^{3+} doped Gd_2O_3 phosphor [7] and the enhanced luminescence of Gd_2O_3:Eu^{3+} phosphors by co-doping with Li^+ ions were also reported [8]. All these results indicated that various co-dopants might exhibit different effects. Some ions may directly act as a flux or sensitizer [9,10] and the others could enter into the host lattice, creating oxygen vacancies or altering the crystal field surrounding the activator, then affecting the luminescence performance of the phosphor [1]. Yu et al. [11] reported that alkali metal ions like LI^+, Na^+ and K^+ co-doped $SrZnO_2$:Eu^{3+} were used to modify the local site symmetry of Eu^{3+} for improving the luminescence efficiency, owing to their chemical nature of low oxidation states and distinct ionic radii. Li et al. [12] studied luminescence properties of $CaAl_2O_4$:Eu^{3+}:R^+ ($R^+ = Li, Na, K$) phosphor prepared by solid state reaction method. Li et al. [13] have studied luminescent properties of $CaMoO_4$:Tb^{3+}:R^+ ($R^+ = Li, Na, K$) by solid state method. The incorporation of R^+ into $CaMoO_4$:Tb^{3+} phosphor could lead to a remarkable increase of PL. Further, the PL intensity depended on the co-doped concentration and intensity increases with R^+ molar concentration until the molar fraction of R^+ squares to Tb^{3+}. The ionic

* Corresponding author.
E-mail address: bhushanvlc@gmail.com (H. Nagabhushana).

1386-1425/$ – see front matter © 2011 Published by Elsevier B.V.
doi:10.1016/j.saa.2011.05.072

radius of Ca^{2+}, Tb^{3+} and Na^{+} is similar. Kuang et al. [14] studied the effect of RE^{3+} (RE^{3+} = Y, La, Gd, Lu) as a co-dopant in $CdSiO_3:Mn^{2+}$ synthesized by solid state method. The ionic radii of the RE^{3+} play an important role in the PL and thermoluminescence (TL) studies. The long lasting phosphorescence was observed in $CdSiO_3:Mn^{2+}:Gd^{3+}$ phosphor. This seems to result from energy transfer of the electrons traps and Gd^{3+} ions to Mn^{2+} ions.

After reviewing the literature, it was observed that, there is a lack of experimental results on the intercommunication between the co-dopants. It is very important to inquire into the characteristics of co-dopants so as to further understand the detailed mechanism of enhanced luminescence, and also help us to look for some more effective co-doping ions. To the best of our knowledge, this problem has been seldom studied. In the present work, various alkali ions such as Li^{+}, Na^{+} and K^{+} were co-doped individually into $Gd_2O_3:Eu^{3+}$ nanophosphors by solution combustion method and a comparative study has been performed. The influence of co-dopants on the enhancement of photoluminescent properties of the phosphors was investigated in detail.

2. Experimental

2.1. Synthesis of M^{+} (M^{+} = Li, Na and K) co-doped $Gd_2O_3:Eu^{3+}$ nanophosphors

The starting chemicals used for the preparation of $Gd_2O_3:Eu^{3+}$ nanophosphors were of analar grade gadolinium nitrate [$Gd(NO_3)_3$], europium nitrate [$Eu(NO_3)_3$], lithium nitrate [$LiNO_3$], sodium nitrate [$NaNO_3$] and potassium nitrate [KNO_3]. The oxalyl dihydrazide [ODH: $C_2H_6N_4O_2$] is used as a fuel for combustion synthesis and was prepared in our laboratory [15]. An aqueous solution containing stoichiometric amounts of gadolinium nitrate, europium nitrate, Li/Na/K nitrate and ODH has been taken in a cylindrical Petri dish of approximately 300 ml capacity. The excess water is allowed to evaporate by heating over a hot plate until a wet powder is left out. Then the Petri dish is introduced into a muffle furnace maintained at $400 \pm 10\,^{\circ}C$. The reaction mixture undergoes thermal dehydration and ignites at one spot with liberation of gaseous products such as oxides of nitrogen and carbon. The combustion of ODH is exothermic and releases the energy required for the synthesis. The combustion propagates throughout the reaction mixture without further need of any external heating, as the heat of reaction is sufficient for the decomposition of redox mixture. The flame temperature was found to be $1000 \pm 10\,^{\circ}C$, which persists for few seconds, and was measured by an optical pyrometer.

2.2. Instruments used

The phase purity of the nanophosphors was examined by Powder X-ray diffractometer (PXRD) (PANalytical X'Pert Pro) using Cu K_α radiation with a nickel filter was used to estimate the crystallinity of the phases. The surface morphology of the product is examined by Scanning Electron Microscopy (SEM) (JEOL JSM 840A). The UV–vis absorption of the samples was recorded on SL 159 ELICO UV–VIS Spectrophotometer. The photoluminescence (PL) measurements was performed on a Shimadzu Spectroflourimeter (Model RF 510) equipped with 150 W Xenon lamp as an excitation source.

3. Results and discussion

It is well known that crystallinity and surface morphology show a strong effect on PL response of phosphor materials. Fig. 1(A) shows the powder X-ray diffraction patterns of as-formed $Gd_2O_3:Eu^{3+}$ (4 mol%) and $Gd_2O_3:Eu^{3+}$ (4 mol%):M^{+} (M^{+} = Li, Na, K) (1 mol%)

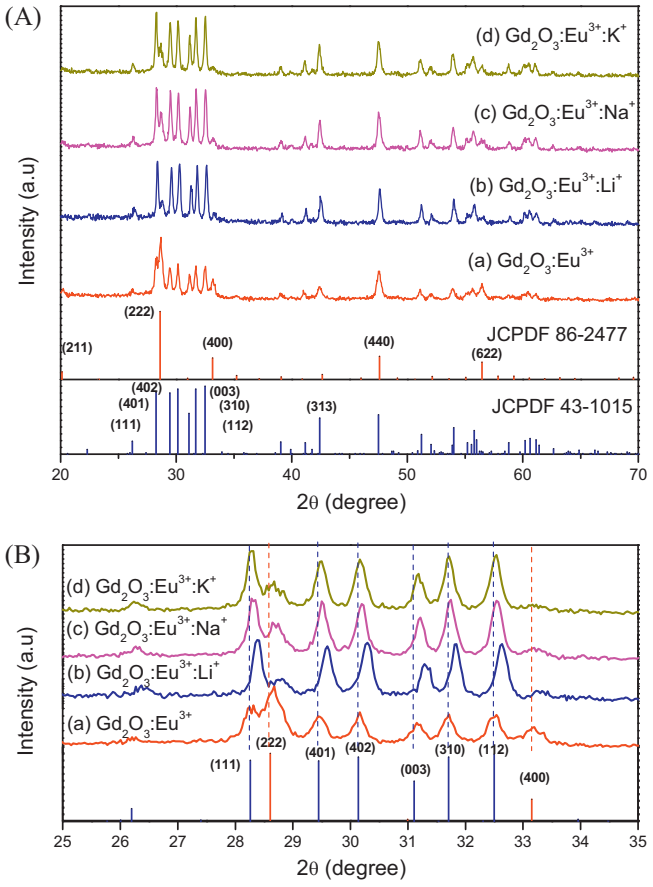

Fig. 1. (A) X-ray diffraction patterns of as-formed (a) $Gd_2O_3:Eu^{3+}$, (b) $Gd_2O_3:Eu^{3+}:Li^{+}$, (c) $Gd_2O_3:Eu^{3+}:Na^{+}$ and (d) $Gd_2O_3:Eu^{3+}:K^{+}$ and (B) magnified view of 2θ values from 25 to 35°.

phosphors. The powder X-ray diffraction results show all the patterns of the samples are consistent with the JCPDS data. The nanopowders show with mixed phase of monoclinic (JCPDS no. 43-1015) and cubic (JCPDS no. 86-2477) structure for $Gd_2O_3:Eu^{3+}$ and alkali ion doped $Gd_2O_3:Eu^{3+}$, respectively. Strong evidence of incorporation of Li^{+}, Na^{+} and K^{+} in $Gd_2O_3:Eu^{3+}$ phase comes from enhanced diffracted intensities. The ratio of the peak values $I_C(2\,2\,2)/I_M(1\,1\,1)$ (intensity of cubic phase to monoclinic phase) is found to 1.43 for $Gd_2O_3:Eu^{3+}$ and 0.43, 0.63 and 0.54 for Li^{+}, Na^{+} and K^{+} co-doped $Gd_2O_3:Eu^{3+}$ samples respectively. The enhanced intensities of the PXRD results of alkali co-doped $Gd_2O_3:Eu^{3+}$ samples suggest better crystallinity compared to $Gd_2O_3:Eu^{3+}$. Further, it is observed that Li^{+} co-doped $Gd_2O_3:Eu^{3+}$ showing maximum diffracted intensity and Li^{+} atom incorporated in to $Gd_2O_3:Eu^{3+}$ lattice substitute for the Gd site.

From the broad PXRD peaks, the crystallite size (d) was calculated using the Debye–Scherer's (D.S.) formula [16].

$$d = \frac{0.9\lambda}{\beta \cos\theta} \tag{1}$$

where d is the average grain size of the crystallites, λ the incident wavelength, θ the Bragg angle and β the diffracted full-width at half-maximum (FWHM) in radians caused by the crystallites. The mean crystallite size calculated from this method is found to be in the range 25–55 nm and it is tabulated in Table 1. It was observed that with the same preparation condition but different impurities could affect the size of the $Gd_2O_3:Eu^{3+}$ nanocrystals. This behavior was in agreement with the crystallite size calculated for different peaks.

Table 1
Various calculated parameters of as formed and heat treated $Gd_2O_3:Eu^{3+}$ samples.

Sample	Asformed			600 °C			700 °C			800 °C			900 °C		
	D–S (nm)	W–H (nm)	Band gap (eV)	D–S (nm)	W–H (nm)	Band gap (eV)	D–S (nm)	W–H (nm)	Band gap (eV)	D–S (nm)	W–H (nm)	Band gap (eV)	D–S (nm)	W–H (nm)	Band gap (eV)
$Gd_2O_3:Eu^{3+}$	29	32	5.44	35	39	5.44	43	47	5.38	52	57	5.27	42	47	5.01
$Gd_2O_3:Eu^{3+}:Li^+$	40	45	5.40	44	50	5.06	43	48	5.19	42	50	5.57	40	46	5.49
$Gd_2O_3:Eu^{3+}:Na^+$	39	44	5.50	39	44	5.53	39	43	5.41	40	45	5.55	39	42	5.52
$Gd_2O_3:Eu^{3+}:K^+$	40	45	5.50	41	46	5.44	42	44	5.43	40	46	5.45	41	45	5.55

D–S = Debye–Scherrer method; W–H = Williamson and Hall method.

The grain size was also estimated from the powder X-ray diffraction line broadening (B) using the analysis described by Williamson and Hall (W–H) method [17].

$$B\cos\theta = \varepsilon(4\sin\theta) + \frac{\lambda}{D} \quad (2)$$

where B (FWHM in radian) is measured for different XRD lines corresponding to different planes, ε is the strain developed and D is the grain size. The equation represents a straight line between 4 $\sin\theta$ (X-axis) and B $\cos\theta$ (Y-axis). The slope of line gives the strain (ε) and intercept (λ/D) of this line on the Y-axis gives grain size (D). It is observed that, the grain size determined from W–H method is slightly higher than that calculated from Debye–Scherrer formula (Table 1). The small variation is due to the fact that in Debye–Scherrer formula strain component is assumed to be zero and observed broadening of diffraction peaks is considered as a result of reducing grain size only. The incorporation of suitable alkali atoms into the lattice of $Gd_2O_3:Eu^{3+}$ improves the crystallinity and better particle formation [8]. However, with inverse of concentration, the excess atoms are aggregated on the grain boundaries due to low solubility of alkali atoms in $Gd_2O_3:Eu^{3+}$. Such surface states would affect the surface kinetics and affect the morphology as seen in $Gd_2O_3:Eu^{3+}$ samples with higher concentration.

With Na^+ and K^+ as additives, the diffraction peaks shift to a smaller angle, but the doping Li^+ ions in $Gd_2O_3:Eu^{3+}$ results in the diffraction peaks shifting to a larger angle. These shifts of the PXRD peaks are attributed to the substitution of the Gd ions by alkali metal ions in host lattice Fig. 1(B). The radii of K^+ (1.33 Å) and

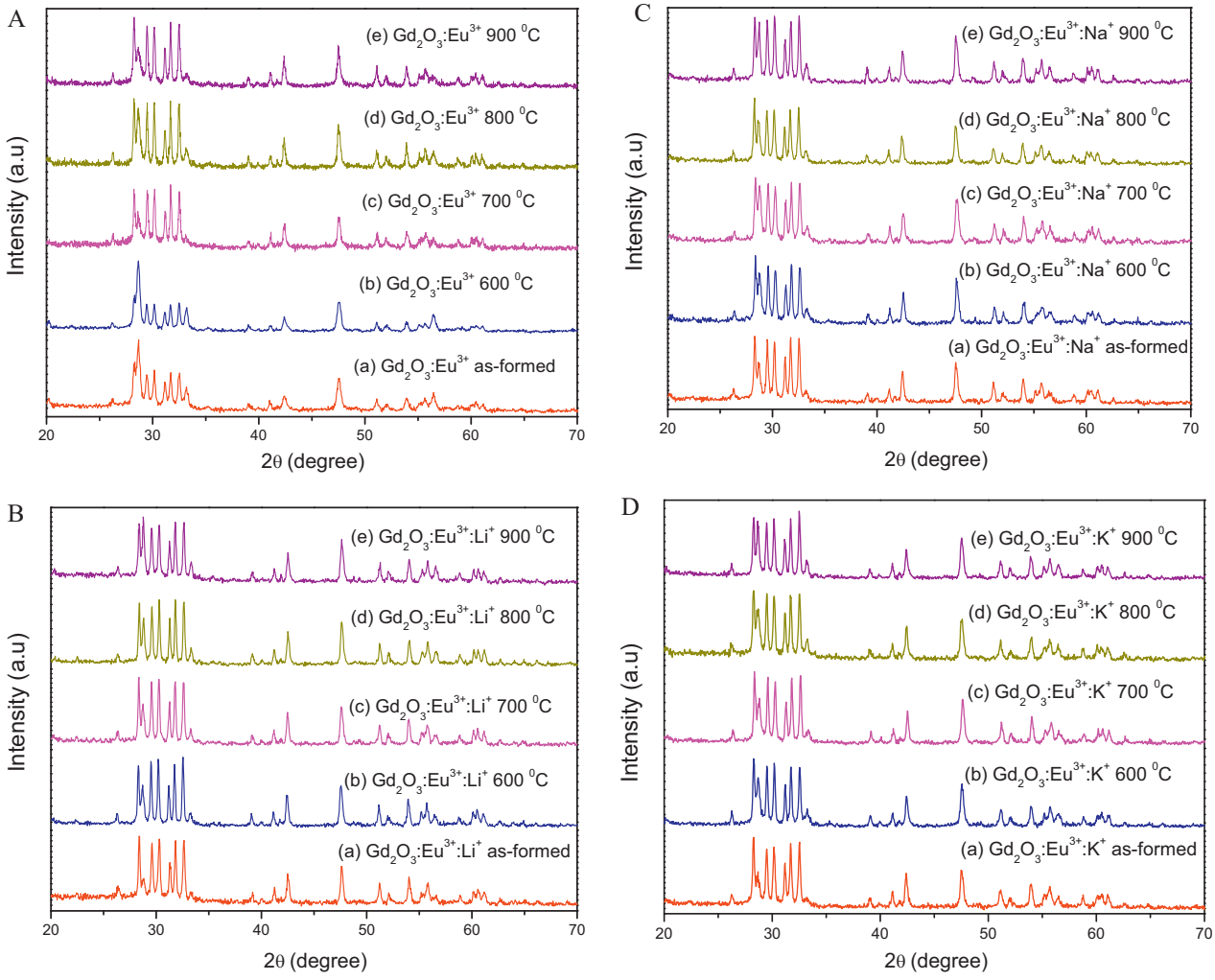

Fig. 2. Powder X-ray diffraction patterns of as-formed and heat treated (600–900 °C for 3 h) in (A) $Gd_2O_3:Eu^{3+}$, (B) $Gd_2O_3:Eu^{3+}:Li^+$, (C) $Gd_2O_3:Eu^{3+}:Na^+$, and (D) $Gd_2O_3:Eu^{3+}:K^+$.

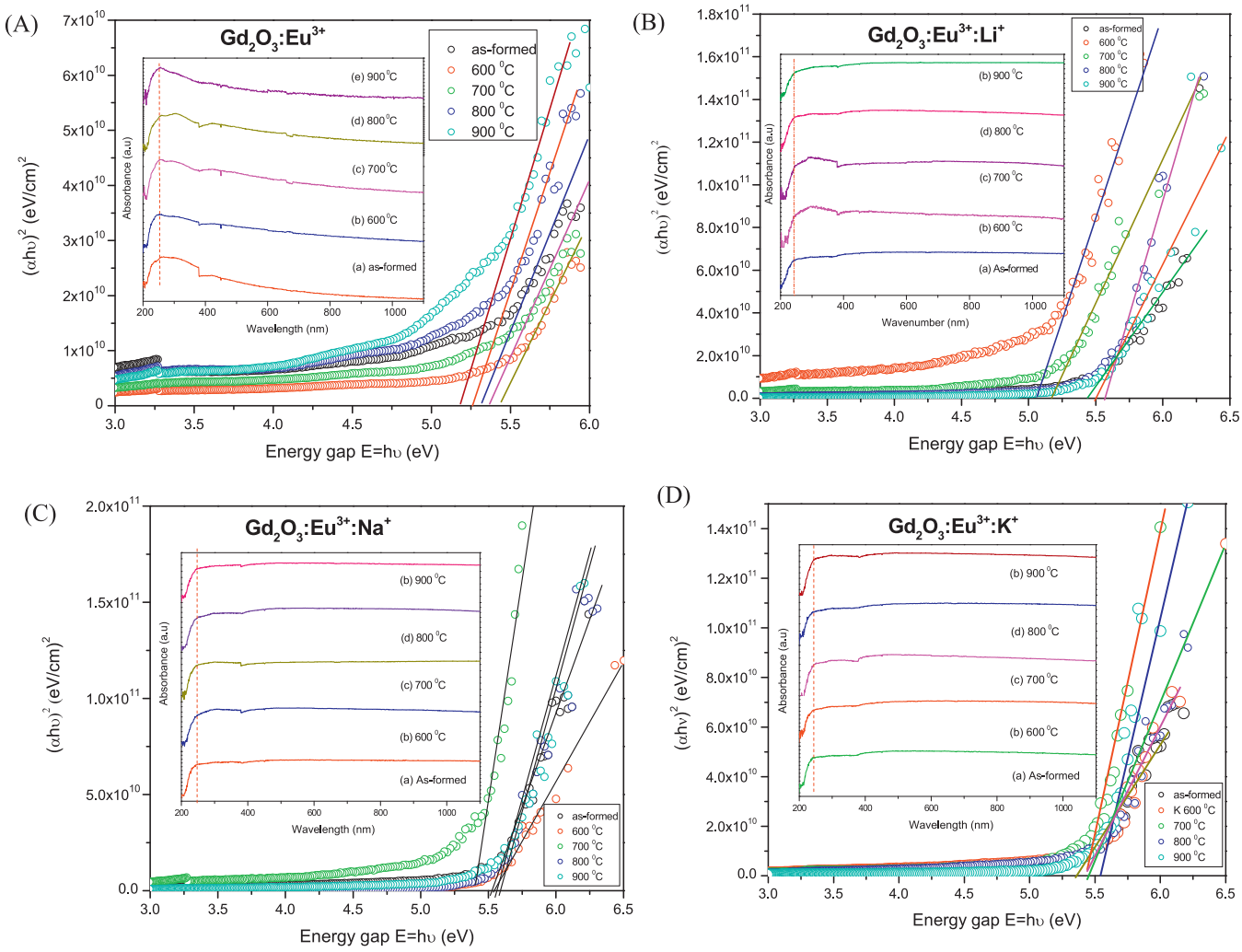

Fig. 3. Energy band gap of as-formed and heat treated (600–900 °C for 3 h) in (A) Gd_2O_3:Eu^{3+}, (B) Gd_2O_3:Eu^{3+}:Li^+, (C) Gd_2O_3:Eu^{3+}:Na^+, and (D) Gd_2O_3:Eu^{3+}:K^+ (inset: UV–vis absorption spectra of as-formed and heat treated (600–900 °C for 3 h) in (A) Gd_2O_3:Eu^{3+}, (B) Gd_2O_3:Eu^{3+}:Li^+, (C) Gd_2O_3:Eu^{3+}:Na^+, and (D) Gd_2O_3:Eu^{3+}:K^+).

Na^+ (0.97 Å) are larger than that of Gd^{3+} (0.94 Å), which results in a smaller angle shift of the peaks in the XRD patterns. However, the radius of Li^+ (0.68 Å) is smaller than that of Gd^{3+} which leads to a larger angle shift of the diffraction peaks. Similar type of results were obtained in Eu^{3+} activated $CaWO_4$ phosphor co-doped with various alkali metal ions (Li^+, Na^+, K^+) and these changes are ascribed due to the cations with different radii and the host compound which results in some distribution of the sub lattice structure around the luminescent center ions [6]. In general, the doped Eu^{3+} and alkaline ions are randomly distributed in the cation sites of the host. These cations with different radii in the host compound can result in some distortions of the sub lattice structure around the luminescent center ions, hence different PL properties are produced [18].

In order to study the effect of calcination temperature on co-doped Gd_2O_3:Eu^{3+} samples, the samples are heated at 600, 700, 800 and 900 °C for 3 h and the PXRD patterns are shown in Fig. 2(A–D), respectively. It is observed that, upon calcinations, the intensity of PXRD peaks increases and it implies that better crystallization has been achieved. This better crystallization can be regarded as the result of flux effect of Li^+, Na^+ and K^+ ions [19].

Added impurities may influence the morphology of a given crystal by participating in the nucleation and growth, in which many overall factors integrate to dominate the process. The requirement of the charge compensation by the substitution dopant ion in Gd site would require different number of dopant ions and related to vacancy states [20]. The morphology of the phosphors was studied by using scanning electron microscopy. The SEM micrographs of Gd_2O_3:Eu^{3+} as-formed and heat treated at 900 °C for 3 h show the phosphors are agglomerated from few microns to a few tens of microns, fluffy and porous in nature. The agglomeration of nanoparticles is usually explained as a common way to minimize their surface free energy. The voids and pores present in the sample are due to the large amount of gases produced during combustion synthesis. Further, the SEM micrographs of Li^+, Na^+, K^+ (1 mol%) co-doped Gd_2O_3:Eu^{3+} phosphor heat treated at 900 °C for 3 h was also studied and show the reduction in agglomeration and better crystallinity.

The UV–vis absorption spectra of Gd_2O_3:Eu^{3+} and Gd_2O_3:Eu^{3+} M^+ (M^+ = Li^+, Na^+, K^+) are shown in inset of Fig. 3(A–D), respectively. All the spectra have strong absorption in the UV spectral region and with some weak peaks in the visible region which are due to intra-4f transitions of Eu^{3+} at lower wavelength. The M^+ co-doped sample exhibits a visible increase of absorbance and an obvious red-shift of the absorption edge compared with the one without M^+ co-doping (Gd_2O_3:Eu^{3+}). It has been known that the position of

the absorption edge is determined by the width of forbidden band with O 2p orbits as the valence band in multi component oxides. Occupation of Gd^{3+} sites by M^+ ions would naturally give rise to a substantial number of oxygen vacancies, which may change the energy band structure and enhance the deformation degree of O 2p orbits and the superposition of the electronic wave functions, and then result in narrowing the forbidden band and shifting the absorption edge to the red.

The optical band gap energy (E_g) of Gd_2O_3:Eu^{3+} and Gd_2O_3:Eu^{3+} M^+ (M^+ = Li^+, Na^+, K^+) (as-formed and heat treated at 600–900 °C for 3 h) are estimated by the method proposed by Wood and Tauc and are shown in Fig. 3(A–D) [21]. According to these authors, the optical band gap is estimated with absorbance and photon energy by the following equation

$$h\nu\alpha \cdot \alpha(h\nu - E_g)^k \quad (3)$$

where α is the absorbance, h is the Planks constant, ν is the frequency, E_g is the optical band gap and k is the constant associated to the different types of electronic transitions $k = 1/2, 2, 3/2, 3$ for direct allowed, indirect allowed, direct forbidden and indirect forbidden transitions, respectively. According to literature [22] the oxides are characterized by an indirect allowed electronic transition and hence, the $k = 2$ value was adopted as standard in Eq. (3). Thus the E_g values was evaluated by extrapolating the linear portion of the curve or tail $[(h\nu\alpha)^{1/k} = 0]$ in the UV–vis absorbance spectra. A plausible explanation for the variations observed in the E_g values can be related to the degree of structural order–disorder in to the lattice, which is able to change the intermediary energy level distribution within the band gap.

The variations in the band gap values might also be due to substitution of Gd ion with smaller Li^+ ion which can induce the shrinking of the host lattice. Whereas, higher, atomic radii (Na^+, K^+) ions occupying the interstitial sites leads to the expansion of the host lattice. Substitution of Na^+ and K^+ in Gd^{3+} sites would naturally generate a substantial number of vacant sites in oxygen ion and then expand the lattice with decrease of crystal density. So the observed lattice expansion with Na^+, K^+ co-doping might be attributed to the weakening of bond strength due to formation of oxygen vacancies. These results indicated that the host lattice shrinks with the radii of Li^+ and then expand when radius of Na^+ and K^+ higher then Gd, while the phosphors heat treated from 600 to 900 °C for 3 h, the absorption spectra show more ordered/crystalline materials. On the basis of this information if the structure becomes more ordered with the heat treated samples, i.e. when the concentration of structural defects (oxygen vacancies, distortions and/or strains in the lattice) is reduced. The presence of intermediary energy levels (deep and shallow holes) is minimized within the optical band gap and consequently, the E_g values increase. As it can be seen, the energy gap values (Table 1) are mainly depends on experimental conditions (heat-treated and processing time) and dopants added. In particular, these key factors can favor or inhibit the formation of structural defects, which are able to control the degree of structural order disorder in the material and consequently, the number of intermediary energy levels within the band gap.

Fig. 4(A–D) shows the photoluminescence excitation (PLE) spectra of as-formed Gd_2O_3:Eu^{3+} and Li^+, Na^+, K^+ co-doped Gd_2O_3:Eu^{3+}, respectively. The PLE spectra consist of a broad excitation band in the range 220–280 nm. The peak nearing 240 nm originates from the excitation of Gd_2O_3 host lattice (HL). Comparing with Gd_2O_3:Eu^{3+}, it is apparent that the CT bands in Li^+, Na^+, K^+ are shifted to ~3 nm which can be assigned to charge transfer band (CTB) of Eu^{3+}–O^{2-} resulting from an electron transfer from the oxygen (O^{2-}) $2p^6$ orbits to the empty 4f states of Eu^{3+} configuration [23]. The CTB of the Li^+, Na^+, K^+ co-doped phosphors was found to be broadened and red shifted when compared to Gd_2O_3:Eu^{3+} phosphor and the amount of red shift increased with increase of atomic radius alkali metal ion.

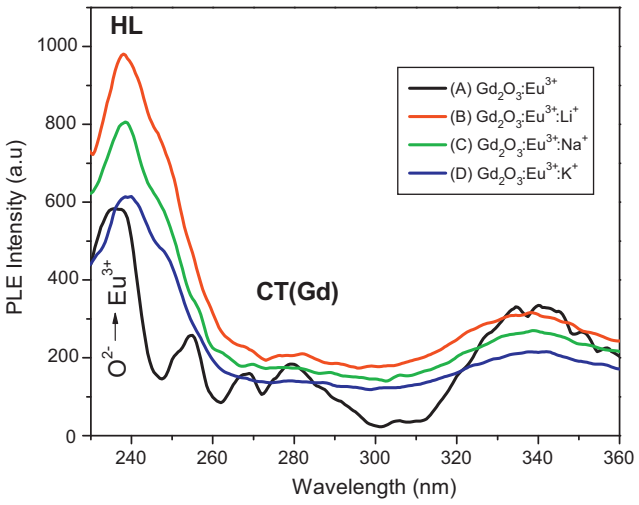

Fig. 4. PLE of as-formed (A) Gd_2O_3:Eu^{3+}, (B) Gd_2O_3:Eu^{3+}:Li^+, (C) Gd_2O_3:Eu^{3+}:Na^+, and (D) Gd_2O_3:Eu^{3+}:K^+.

The PL emission spectra of as-formed Gd_2O_3:Eu^{3+} and Li^+, Na^+, K^+ co-doped Gd_2O_3:Eu^{3+} are shown in Fig. 5. It consists of sharp and intense bands with peak positions at 594, 612 and 628 nm along with a weak band with peak position at 582 nm in the 550–650 nm spectral regions. The weak emission band observed at 582 nm can be assigned to the $^5D_0 \rightarrow {}^7F_0$ transition, the band obtained at 594 nm can be assigned to $^5D_0 \rightarrow {}^7F_1$ magnetic dipole transition and the other two emissions observed at 612 and 623 nm can be assigned to $^5D_0 \rightarrow {}^7F_2$ indicated electric dipole transition of Eu^{3+} ions. Among these emission transitions, the magnetic dipole transition is independent of local environment while the electric dipole transition is hypersensitive to the symmetry of local environment around Eu^{3+} ions. The intensity distribution of the $^5D_0 \rightarrow {}^7F_J$ transitions among different J ($J = 0, 1, 2, 3$) levels depends on the symmetry of the local environment around Eu^{3+} ions and can be described in terms of Judd–Ofelt theory [24,25]. According to the selection rules, magnetic dipole transition is permitted and electric dipole is forbidden, but for some cases in which local symmetry of the activators without an inversion center, the parity forbidden is partially permitted, such as Eu^{3+} ion occupying C_2 cites in Y_2O_3:Eu^{3+} [26].

The emission intensity of Gd_2O_3:Eu^{3+} and Li^+, Na^+, K^+ co-doped Gd_2O_3:Eu^{3+} phosphor is dominated by the $^5D_0 \rightarrow {}^7F_1$ transition peak observed at 612 nm. The PL measurements indicated no

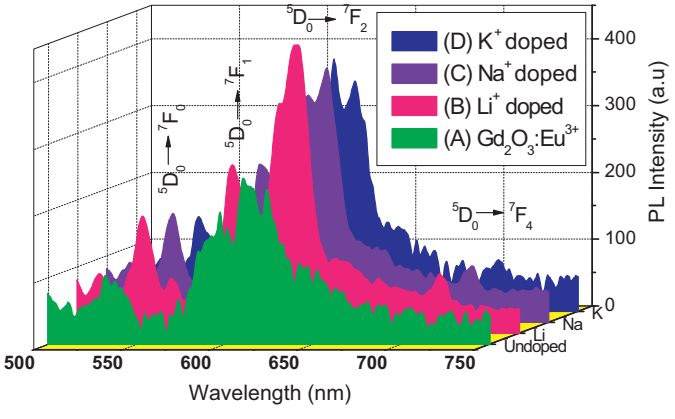

Fig. 5. PL of as-formed (A) Gd_2O_3:Eu^{3+}, (B) Gd_2O_3:Eu^{3+}:Li^+, (C) Gd_2O_3:Eu^{3+}:Na^+, and (D) Gd_2O_3:Eu^{3+}:K^+.

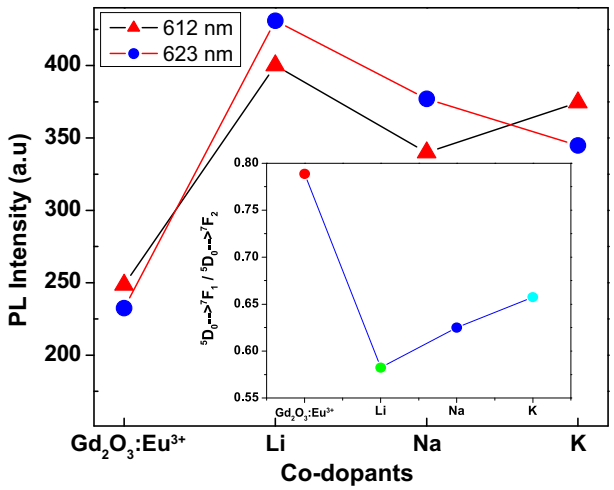

Fig. 6. Variation in PL intensity of 612 and 623 nm peaks in Gd_2O_3:Eu^{3+} and Li^+, Na^+ and K^+ co-doped samples (inset: variation of $^5D_0 \rightarrow {}^7F_1/{}^5D_0 \rightarrow {}^7F_2$ ratio for Gd_2O_3:Eu^{3+} and Li^+, Na^+ and K^+ co-doped samples).

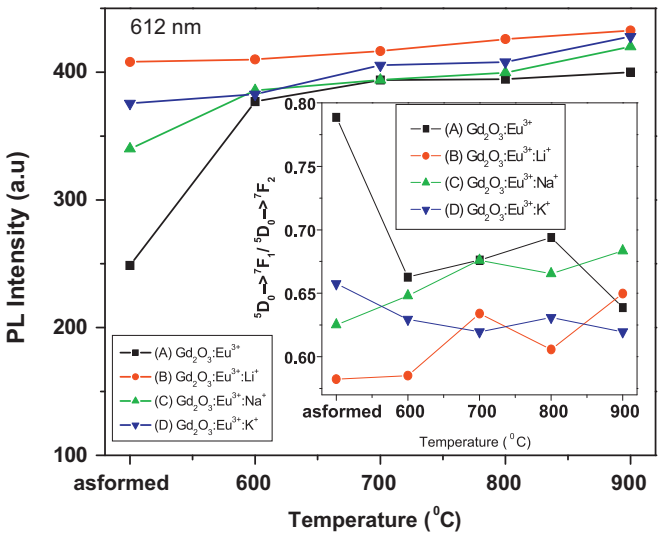

Fig. 7. Variation in PL intensity (as formed and heat treated at 600–900 °C for 3 h) of red emission (612 nm) peak in Gd_2O_3:Eu^{3+} and Li^+, Na^+ and K^+ co-doped samples (inset: variation of $^5D_0 \rightarrow {}^7F_1/{}^5D_0 \rightarrow {}^7F_2$ ratio (as-formed and heat treated at 600–900 °C for 3 h) in Gd_2O_3:Eu^{3+} and Li^+, Na^+ and K^+ co-doped Gd_2O_3:Eu^{3+} samples.

significant change in the emission shape or position except PL intensity. The integral intensity of the emission spectrum of Li^+, Na^+, K^+ co-doped samples is increased by a factor of 1.64, 1.59 and 1.51 when compared to that of Gd_2O_3:Eu^{3+} phosphor. This fact indicates that the charge transfer from the O^{2-} to Eu^{3+} is enhanced and more efficient with incorporation of Li^+, Na^+ and K^+ ions and these ions acted as an intermediator for transfer of excitation energy from the host lattice to the activator [27], which leads to enhancement of PL. the improvement of PL intensity with Li^+, Na^+, K^+ may be attributed to the improved crystallinity which leads to higher oscillator strength for the optical transitions [28], as well as enlarged grain sizes inducing lower scattering loss. Further, substitution of Li^+, Na^+, K^+ in to Gd^{3+} sites would eventually a substantial number of oxygen vacancies on the surface of the phosphor. These oxygen vacancies might act as sensitizer for the energy transfer from host to Eu^{3+} ion due to the strong mixing of charge transfer states and enhances the luminescence intensity [29].

The PL intensity in as-formed Li^+ co-doped samples is higher when compared to as-formed Gd_2O_3:Eu^{3+} and Na^+ and K^+ co-doped samples (Fig. 6). Further, it is observed that the ratio of $^5D_0 \rightarrow {}^7F_1/{}^5D_0 \rightarrow {}^7F_2$ is called as symmetric ratio (inset of Fig. 8), gives a measure of the degree of distortion from inversion symmetry of the local environment surrounding the Eu^{3+} ions in the host matrix. The symmetric ratio is lower for Li^+ co-doped samples when compared to Gd_2O_3:Eu^{3+} and Na^+, K^+ co-dopants.

It is well known that relative intensity of $^5D_0 \rightarrow {}^7F_1$ and $^5D_0 \rightarrow {}^7F_2$ transitions strongly depended on the local symmetry of Eu^{3+} ions. Subsequently, when Eu^{3+} ion occupy the cites with inversion centers, the $^5D_0 \rightarrow {}^7F_1$ transition should be relatively strong; while, the $^5D_0 \rightarrow {}^7F_2$ transition is parity forbidden and should be very weak. The effect of enhanced luminescence is weak if the size of the co-doping ion is larger than that of Gd^{3+}. It could be regarded that incorporation of the co-doping ions in host lattice will introduce a stress in the neighboring of the co-dopant, i.e. Gd^{3+} or Eu^{3+} due to the Eu^{3+} ions incorporated in to the Gd^{3+} sites [30]. Thus, the crystal field surrounding the Eu^{3+} ions would be altered. The sites offered for Eu^{3+} ions will have more reduced symmetry which is able to lift the parity selection rule and increase transition possibility of electron, and then result in an increase of PL intensity [31]. Additionally the local distribution will be enhanced with the increase of the positive size co-dopant and the host cation [32]. To further understand the effect of co-dopant on enhanced luminescence emission emphasis will be upon the Li^+, Na^+, K^+ co-dopant samples in the following discussion. The co-doping ions may act as flux directly [19] or enter the host lattice at substitutional sites, creating the oxygen vacancy, which acts as a sensitizer for promotion of the energy transfer [9].

In the present study, all the three types of alkali metal ions are able to enhance the luminescence of the phosphor and among them co-doped with Li^+ show the highest red emission intensity. The ionic radius of the Li^+ is 0.68 Å which is smaller than that of Gd (0.94 Å), while Na^+ and K^+ 0.97 Å and 1.33 Å which is bigger than Gd^{3+} site. The evident change of the emission intensity is due to the difference in the ionic radii of the alkali metal ions. Thus Li^+ is expected to cause less distortion in the crystal structure of the phosphors. The alkali metal ions such as Li^+, Na^+, K^+ have the valance electronic configurations of noble gases. With the ionic radii increasing; the difference of ionic radii gives rise to the diversity of the sub-lattice structure around the luminescent center ions, which influences the spin orbit coupling and crystal field of Eu^{3+} ions [33]. The difference in ionic radii of alkali metal ions Eu^{3+} and Gd^{3+} ions will slightly influence the coordination conditions for Eu^{3+} when alkali metal ions were co-doped in to Gd_2O_3:Eu^{3+}. In consequence, the Eu–O distance may change slightly and the peaks and relative intensities of excitation and emission for Gd_2O_3:Eu^{3+} M^+ (M^+ = Li, Na, K) would be different with different alkali ions co-doping.

It could be believed that alkali metal ions incorporation introduces some bound electron-hole pairs. In Gd_2O_3:Eu^{3+}, alkali metal ions (Li^+, Na^+, K^+) substitute for Gd^{3+} create point defects such as oxygen vacancies. The radius and charge number of alkali metal ions (Li^+, Na^+ and K^+) are much different from those of Gd^{3+} lattice of Gd_2O_3:Eu^{3+} will cause the information of bond electron-hole pair. The PL spectra of Gd_2O_3:Eu^{3+} and Li^+, Na^+, K^+ co-doped Gd_2O_3:Eu^{3+} (as-formed and heat treated at 600–900 °C) phosphors excited with 243 nm was also studied narrow emission peaks are observed which are due to the shielding effect of 4f electrons by 5s and 5p electrons in the outer shells of the Eu^{3+} activator. The strongest emission peaks located at 612 nm is assigned to $^5D_0 \rightarrow {}^7F_2$ transition of Eu^{3+} ions, and the peaks at around 593 and 705 nm are due to $^5D_0 \rightarrow {}^7F_1$ and $^5D_0 \rightarrow {}^7F_4$ transition, respectively. It is obvious that different co-dopants have different contributions on PL intensity of Gd_2O_3:Eu^{3+} phosphor and the intensity is improved remarkably by co-doping with Li^+, Na^+ and K^+. The incorporation of co-doping ions in the host lattice is associated with the mismatches in size

and electro negativity between co-dopant and host cation. Further it is evident that PL intensity of Gd_2O_3:Eu^{3+} phosphor is enhanced drastically by the co-doping ion whose radius is smaller than that of Gd^{3+} ion. Further, it is observed that in all the cases, the PL intensity increases as calcinations temperature increases.

Fig. 7 shows the PL intensity (as-formed and heat treated at 600–900 °C for 3 h) of Gd_2O_3:Eu^{3+} and Li^+, Na^+, K^+ co-doped Gd_2O_3:Eu^{3+}samples, respectively. It is observed that PL intensity in Li^+ co-doped Gd_2O_3:Eu^{3+} is higher than compared that of Gd_2O_3:Eu^{3+} and Na^+, K^+ co-doped Gd_2O_3:Eu^{3+}. Further, the symmetric ratio ($^5D_0 \rightarrow {}^7F_1/{}^5D_0 \rightarrow {}^7F_2$) in Li^+ co-doped Gd_2O_3:Eu^{3+} is lower than that of Gd_2O_3:Eu^{3+} and Na^+, K^+ co-doped Gd_2O_3:Eu^{3+}.

4. Conclusions

Gd_2O_3:Eu^{3+} and the alkali metal ions (M = Li^+, Na^+, K^+) co-doped nanophosphors was synthesized by combustion method in a short time. PXRD results confirm that Gd_2O_3:Eu^{3+} nanopowders exhibit mixed phase of monoclinic and cubic. The incorporation of Li^+, Na^+ and K^+ in Gd_2O_3:Eu^{3+} phase is evident from the enhanced diffracted intensities. The effect of Li^+, Na^+, K^+ co-doping on the PL properties of Gd_2O_3:Eu^{3+} phosphors is discussed. The results indicate that the PL intensity of Gd_2O_3:Eu^{3+} was improved remarkably by co-doping with Li^+, whose ionic radius is less than that of Gd^{3+} and the intensity decreases with greater than that of Gd^{3+}. Enhanced luminescence mainly regarded as that result of a suitable local distortion of the crystal field surrounding Eu^{3+} activator in Gd_2O_3:Eu^{3+}. This local distortion is closely related to effective ionic radius.

Acknowledgements

The authors are grateful to TEQIP Lab (Chemistry) of M.S. Ramaiah Institute of Technology, Bangalore for providing facilities for preparation of materials. One of the authors N.D. acknowledges Dr. N.D.N. Prasad, HOD, B.M.S. Institute of Technology, Bangalore for the support and encouragement. The author H.N. thanks Dr. S.C. Sharma, Vice-chancellor, Tumkur University, Tumkur, for constant encouragement and support.

Appendix A. Supplementary data

SEM micrographs of as-formed Gd_2O_3:Eu^{3+}, co-doped and heat treated phosphors; PL emission spectra of as-formed Gd_2O_3:Eu^{3+}, and heat treated co-doped (Li^+, Na^+ and K^+) phosphors at 600–900 °C (for 3 h).

Supplementary data associated with this article can be found, in the online version, at doi:10.1016/j.saa.2011.05.072.

References

[1] X. Liu, K. Han, M. Gu, L. Xiao, C. Ni, S. Huang, B. Liu, Solid State Commun. 142 (2007) 680–684.
[2] E.J. Bosze, G.A. Hirata, L.E. Shea-Rohwer, J. McKittrick, J. Lumin. 104 (2003) 47–54.
[3] J.H. Jeong, J.S. Bae, S.S. Yi, J.C. Park, Y.S. Kim, J. Phys.: Condens. Matter 15 (2003) 567–574.
[4] G. Blasse, B.C. Grabmaier, Luminescent Materials, Springer, New York, 1994.
[5] J. Li, Y. Wang, B. Liu, J. Lumin. 130 (2010) 981–985.
[6] S. Shi, J. Gao, J. Zhou, Opt. Mater. 30 (2008) 1616–1620.
[7] N. Dhananjaya, H. Nagabhushana, B.M. Nagabhushana, R.P.S. Chakradhar, C. Shivakumara, B. Rudraswamy, Physica B 405 (2010) 3795–3799.
[8] N. Dhananjaya, H. Nagabhushana, B.M. Nagabhushana, B. Rudraswamy, C. Shivakumara, R.P.S. Chakradhar, J. Alloys Compd. 509 (2011) 2368–2374.
[9] S.S. Yi, J.S. Bae, K.S. Shim, J.H. Jeong, J.C. Park, P.H. Holloway, Appl. Phys. Lett. 84 (2004) 353–355.
[10] L.S. Chi, R.S. Liu, B.J. Lee, J. Electrochem. Soc. 152 (2005) J93–J98.
[11] X. Yu, X. Xu, C. Zhou, J. Tang, X. Peng, S. Yang, Mater. Res. Bull. 41 (2006) 1578–1583.
[12] G. Li, Y. Lai, T. Cui, H. Yu, D. Liu, S. Gan, Mater. Chem. Phys. 124 (2010) 1094–1099.
[13] X. Li, Z. Yang, L. Guan, J. Guo, Y. Wang, Q. Guo, J. Alloys Compd. 478 (2009) 684–686.
[14] J. Kuang, Y. Liu, B. Lei, J. Lumin. 118 (2006) 33–38.
[15] K.C. Patil, M.S. Hegde, S.T. Tanu Rattan, Aruna, Chemistry of Nanocrystalline. Oxide Materials, Combustion synthesis, Properties and Applications, World. Scientific Publishing Co. Pt. Ltd., UK, 2008.
[16] P. Klug, L.E. Alexander, X-ray Diffraction Procedure, Wiley, New York, 1954.
[17] G.K. William, W.H. Hall, Acta Metall. 1 (1953) 22–31.
[18] J.P.M. Van Vliet, G. Blasse, L.H. Brixner, J. Solid State Chem. 76 (1988) 160–166.
[19] D.B. Hedden, C.C. Torardi, W. Zegarski, J. Solid State Chem. 118 (1995) 419–421.
[20] K. Jayanthi, S. Chawla, K.N. Sood, M. Chhibara, Sukvir Singh, Appl. Surf. Sci. 255 (2009) 5869–5875.
[21] J. Tauc, in: F. Abeles (Ed.), Optical Properties of Solids, North-Holland, Amsterdam, 1970.
[22] X. Liu, F. Zhou, M. Gu, S. Huang, B. Liu, C. Ni, Opt. Mater. 31 (2008) 126–130.
[23] B. Liu, M. Gu, X. Liu, C. Ni, D. Wang, L. Xiao, R. Zhang, J. Alloys Compd. 440 (2007) 341–345.
[24] B.R. Judd, Phys. Rev. 127 (1962) 750–761.
[25] G.S. Ofelt, J. Chem. Phys. 37 (1962) 511–519.
[26] Z. Wei, L. Sun, C. Liao, J. Yin, X. Jiang, C. Yan, S. Lü, J. Phys. Chem. B 106 (2002) 10610–10617.
[27] J.H. Lee, M.H. Heo, S.J. Kim, S. Nahm, K. Park, J. Alloys Compd. 473 (2009) 272–274.
[28] L. Sun, C. Quian, C. Liao, X. Wang, C. Yan, Solid State Commun. 119 (2001) 393–400.
[29] J.H. Jeong, H.K. Yang, K.S. Shim, Y.R. Jeong, B.K. Moon, B.C. Choi, J.S. Bae, S.S. Yi, J.H. Kim, Appl. Surf. Sci. 253 (2007) 8273–8277.
[30] A.A. Kaplyanskii, R.M. Macfarlane, Spectroscopy of Solids Containing Rare Earth Ions, North-Holland, Amsterdam, 1987.
[31] K.E. Waldrip, J.S. Lewis, Q. Zhai, M.P. Lambers, M.R. Divison, P.H. Holloway, S.S. Sun, J. Appl. Phys. 89 (2001) 1664–1670.
[32] E. Antic-Fidancev, J. Holsa, M. Lastusaari, A. Lupei, Phys. Rev. B 64 (2001) 195108–195115.
[33] S.K. Shi, J. Gao, ZhouF J., Opt. Mater. 30 (2008) 1616–1620.